Classical gluon radiation in ultrarelativistic nucleus-nucleus collisions

Yuri V. Kovchegov
Department of Physics, Columbia University, New York, New York 10027

Dirk H. Rischke
Department of Physics, Duke University, Box 90305, Durham, North Carolina 27708-0305
(Received 1 April 1997)

The classical Yang-Mills equations are solved perturbatively in covariant gauge for a collision of two ultrarelativistic nuclei. The nuclei are taken as ensembles of classical color charges on eikonal trajectories. The classical gluon field is computed in coordinate space up to cubic order in the coupling constant g. We construct the Feynman diagrams corresponding to this field and show the equivalence of the classical and diagrammatic approaches. An argument is given which demonstrates that at higher orders in g the classical description of the process breaks down. As an application, we calculate the energy, number, and multiplicity distributions of produced soft gluons and reproduce earlier results by Gunion and Bertsch and by Kovner, McLerran, and Weigert. [S0556-2813(97)07008-8]

PACS number(s): 25.75.−q, 12.38.Aw, 12.38.Bx, 24.85.+p

I. INTRODUCTION

Ultrarelativistic heavy-ion collisions ($\sqrt{s}\sim 200A$ GeV) at the Relativistic Heavy Ion Collider (RHIC) at Brookhaven aim towards an understanding of the properties of nuclear matter under extreme conditions [1]. It was argued that the extraordinarily high energy and particle number densities reached in central nuclear collisions at RHIC, $\epsilon\sim 10$–20 GeV fm^{-3}, $dN/dy\sim 1000$ [2], could lead to rapid (local) thermalization of matter [3] and thus to the creation of the so-called quark-gluon plasma (QGP) [4], a state predicted by finite temperature lattice QCD calculations [5], where chiral symmetry is restored and quarks and gluons are deconfined.

In order to assess whether this state can actually be formed in an ultrarelativistic nuclear collision one has to gain a better understanding of the initial conditions and, at these energies predominantly hard, parton-parton scattering processes in the early stage preceding (local) thermodynamical equilibrium. While event generators based on individual parton-parton scattering processes [6] have been developed, their respective predictions for the range of accessible energy and particle number densities differ widely.

One of the main reasons is the poor understanding of the initial conditions for the nuclear reaction. Recently, McLerran and Venugopalan have made considerable progress in a classical approach [7] to construct the gluon field at small values of x. Their treatment is somewhat similar to the approach used by Mueller for constructing the wave function and gluon structure function of a heavy quarkonium state [8]. At small x, the nucleonic structure is dominated by gluons, and thus a proper description of gluon dynamics in this kinematic region is vital for understanding the initial conditions and the subsequent preequilibrium stage in nuclear collisions.

The McLerran-Venugopalan model [7] considers a very large nucleus moving at ultrarelativistic velocity, which consequently appears in the laboratory frame as a ''pancake'' in the transverse plane. It is assumed [7] that due to the large size of the nucleus the (transverse, two-dimensional) color charge density $\rho(\underline{x})$ is large (i.e., in a higher-dimensional representation of the color algebra) so that in a certain kinematic region the soft gluon field produced by these color charges is effectively *classical*, and can thus be obtained by solving the *classical* Yang-Mills equations of motion. This field can then be used to compute the gluon distribution function. Quantum effects can be implemented as corrections to the classical field.

The kinematic region for which this approximation is valid is given by the following consideration [7,9]: The strong coupling constant $\alpha_S\equiv g^2/4\pi$ should be small, and therefore the typical gluon transverse momenta in the problem should satisfy $k_\perp \gg \Lambda_{\rm QCD}$. On the other hand, the gluon transverse momenta should be sufficiently ''soft,'' such that the gluons do not resolve individual color charges but couple to the classical color charge density. At very high transverse momenta quantum effects become important. Therefore, we have to limit ourselves to the region where $k_\perp \ll \mu$, with μ^2 being the average color charge density squared. The momentum fraction x of the gluons should be small enough so that the nucleus appears coherent in the longitudinal direction.

To facilitate the inclusion of quantum corrections, the authors of [7] searched for the classical gluon field of such a nucleus in the light-cone gauge. The solution of the equations of motion requires one to take the longitudinal extension of the nucleus into account; i.e., one must not take the nucleus to be infinitely thin in the longitudinal direction, as was assumed originally in [7]. The classical field of a single ultrarelativistic nucleus is the non-Abelian Weizsäcker-Williams field. It was computed in [10,11]. In the approach pursued in [11] the nucleus was assumed to be an ensemble of nucleons consisting of pointlike (valence) color charges. Instead of a smooth two-dimensional color charge density $\rho(\underline{x})$, this quantity is a sum of δ functions in [11]. The limit of applicability of the classical approximation, as well as the structure of the non-Abelian Weizsäcker-Williams field in terms of Feynman diagrams, has been discussed in [12]. That

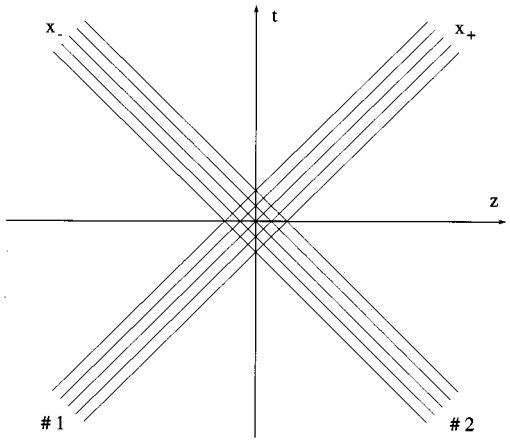

FIG. 1. The nuclear collision as envisaged here (for details, see text).

model also allowed for an explicit calculation of the average color charge density squared μ^2.

One of the goals of the approach of McLerran and Venugopalan is to obtain the Balitsky-Fadin-Kuraev-Lipatov (BFKL) equation for the structure function of soft gluons and, if possible, derive corrections to this equation which account for nuclear shadowing. Recently, a first step in this direction has been made: The BFKL equation was obtained via a renormalization group approach [13].

A collision of two ultrarelativistic nuclei of the type advertised in [7] was considered in [9]. The Yang-Mills equations were simplified assuming that the solution for the gluon field in the forward light cone is boost invariant. The equations were then solved perturbatively to first order in the corrections to the Abelian solution in the gauge $x_-A_+ + x_+A_- = 0$ [where $x_\pm = (t \pm z)/\sqrt{2}$ and $A_\pm = (A^0 \pm A^z)/\sqrt{2}$ are the light-cone components of the gluon field].

In this paper, we also focus on an ultrarelativistic nuclear collision, but we employ the approach of [11] to describe the nuclei. Each nucleus is moving with the speed of light. The nuclei are taken to be ensembles of nucleons, consisting of pointlike color charges (valence quarks). The first nucleus is supposed to move in the ''+'' direction, the second in the ''−'' direction; see Fig. 1. In contrast to [7,9], they *do* have a longitudinal extension; i.e., a color charge in nucleus 1 has a fixed x_- component x_{-i}, which is different for each charge, $x_{-i} \neq x_{-k}, i \neq k$, and similar for nucleus 2, where the charges have fixed x_+ components y_{+j} (of course, all charges have different transverse coordinates $\underline{x}_i, \underline{y}_j$ as well).

During the collision, we assume the momenta of the charges to remain unchanged (eikonal trajectories). This is certainly justified, since we consider the initial momenta of the charges to be rather large (if not infinite). The nuclei just pass through each other and continue their motion along the light cone (see Fig. 1). As in [9], we also solve the classical Yang-Mills equations perturbatively to first order in the corrections to the Abelian solution and obtain the classical, radiated gluon field. In contrast to [9], however, we shall work *exclusively* in the covariant (Lorentz) gauge. The advantage of this gauge is that, for the case of a single ultrarelativistic nucleus, the classical gluon field is identical to the solution of the corresponding Abelian problem [11]. Moreover, as will be shown below, for the collision of two nuclei, one can easily relate the classical solution to that of a diagrammatic approach in terms of the usual Feynman rules in covariant gauge (such rules do not exist in momentum space for the gauge chosen in [9]).

The outline of the paper is as follows. In Sec. II we discuss the lowest order solution to the Yang-Mills equations. This is just the solution to the corresponding Abelian problem; i.e., the fields generated by the color charges in the nuclei are simply superposed and no real gluons are produced. In Sec. III we find the classical field to order g^3. This is the first (and lowest) order correction to the Abelian solution. We shall derive an explicit expression for the field in coordinate space. We establish the correspondence between this classical result and a particular set of Feynman diagrams. This proves that, at this order, the classical field is the (major) source of soft gluon production. We shall argue that at higher orders the classical description will fail, since already at order g^5 nonclassical contributions to the gluon field become important. In Sec. IV we calculate energy, number, and multiplicity distributions of the produced gluons. As expected, their form is similar to the one found previously in [9,14]. However, the prefactor of our result is different from that in [9], while it agrees with the result of [14] and [19].

Our units are $\hbar = c = 1$, and the metric tensor is $g^{\mu\nu} = \mathrm{diag}(+,-,-,-)$. Light-cone coordinates are defined in the usual way, $a_\pm \equiv (a^0 \pm a^z)/\sqrt{2}, \partial_\mp \equiv \partial/\partial x_\pm$. The notation for transverse vectors is $\underline{a} = (a^x, a^y)$.

II. CLASSICAL SOLUTION TO LOWEST ORDER IN THE COUPLING CONSTANT

We consider two nuclei with mass numbers A_1, A_2 moving towards each other with ultrarelativistic velocities $v_{1,2} \simeq \pm 1$ along the z axis (cf. Fig. 1). The nuclei are taken as ensembles of nucleons [11]. In order to simplify the color algebra each ''nucleon'' consists of a quark-antiquark pair. These valence quarks and antiquarks are confined inside the nucleons (visualized as spheres of equal radius in the rest frame of each nucleus). In order to construct the solution, nucleons inside the nucleus and valence charges inside the nucleons are assumed to be ''frozen''; i.e., they have definite light-cone (and transverse) coordinates which, due to our assumption of eikonal trajectories for the individual charges, will not change throughout the calculation. We label the coordinates of the quarks in nucleus 1 by $x_{-i}, \underline{x}_i, i = 1, \ldots, A_1$, and those of nucleus 2 by $y_{+j}, \underline{y}_j, j = 1, \ldots, A_2$. Antiquark coordinates follow this notation with an additional prime. As in [11], the nuclei are supposed to be sufficiently ''dilute,'' such that the distance between the nucleons is much larger than the nucleon's size.

The goal of this section is to solve the classical QCD equations of motion,

$$D_\mu F^{\mu\nu} = J^\nu, \tag{1}$$

to lowest order in the strong coupling constant (our convention for the covariant derivative is $D_\mu \equiv \partial_\mu - ig[A_\mu, \cdot]$). We

shall work exclusively in the covariant gauge ($\partial_\mu A^\mu = 0$). In this gauge, the equations of motion (1) can be cast into the form

$$\Box A^\mu = J^\mu + ig[A_\nu, \partial^\nu A^\mu + F^{\nu\mu}], \tag{2}$$

where $\Box$ is the d'Alembertian operator. In this form, it is easy to solve the equations perturbatively, as will be outlined in the following.

To lowest order in g, i.e., order g, the commutator term on the right-hand side of Eq. (2) does not contribute, since the field itself is already of this order [see Eq. (4) below]. To this order and in covariant gauge, the classical current can be taken as a sum of the currents for each individual nucleus, as given in [11]:

$$J_+^{(1)} = g\sum_{i=1}^{A_1} T^a(T_i^a)[\,\delta(x_- - x_{-i})\,\delta(\underline{x}-\underline{x}_i) - \delta(x_- - x'_{-i})\,\delta(\underline{x}-\underline{x}'_i)], \tag{3a}$$

$$J_-^{(1)} = g\sum_{j=1}^{A_2} T^a(\tilde{T}_j^a)[\,\delta(x_+ - y_{+j})\,\delta(\underline{x}-\underline{y}_j) - \delta(x_+ - y'_{+j})\,\delta(\underline{x}-\underline{y}'_j)], \tag{3b}$$

$$\underline{J}^{(1)} = 0, \tag{3c}$$

where T^a are the generators of SU(N_c), and (T_i^a) and ($\tilde{T}_j^a$) are color matrices which represent the color charge of the quark in the color space of nucleon i in the first and nucleon j in the second nucleus, respectively (see [11]). The current (3) takes into account that antiquarks have the opposite color charge and thus ensures color neutrality for each nucleon.

The classical gluon field satisfying the Yang-Mills equations for a *single* ultrarelativistic nucleus of our type was found in [11]. To lowest order in the coupling constant the solution of Eq. (2) for two nuclei will be just a sum of the solutions for single nuclei, since the equations of motion are Abelian ($\Box A_\mu^{(1)} = J_\mu^{(1)}$), and thus linear. Therefore, as one readily confirms by an explicit calculation, the solution of the Yang-Mills equations to order g is [11]

$$A_+^{(1)} = -\frac{g}{2\pi}\sum_{i=1}^{A_1} T^a(T_i^a)[\,\delta(x_- - x_{-i})\ln(|\underline{x}-\underline{x}_i|\lambda) - \delta(x_- - x'_{-i})\ln(|\underline{x}-\underline{x}'_i|\lambda)], \tag{4a}$$

$$A_-^{(1)} = -\frac{g}{2\pi}\sum_{j=1}^{A_2} T^a(\tilde{T}_j^a)[\,\delta(x_+ - y_{+j})\ln(|\underline{x}-\underline{y}_j|\lambda) - \delta(x_+ - y'_{+j})\ln(|\underline{x}-\underline{y}'_j|\lambda)], \tag{4b}$$

$$\underline{A}^{(1)} = 0, \tag{4c}$$

where λ enters as an infrared cutoff. In a sense, it acts as a gauge parameter that sets the scale of the gauge potential. The associated field strength tensor is independent of λ,

$$F_{+-}^{(1)} = 0, \tag{5a}$$

$$F_{+\perp}^{(1)} = \frac{g}{2\pi}\sum_{i=1}^{A_1} T^a(T_i^a)\left(\,\delta(x_- - x_{-i})\frac{\underline{x}-\underline{x}_i}{|\underline{x}-\underline{x}_i|^2} - \delta(x_- - x'_{-i})\frac{\underline{x}-\underline{x}'_i}{|\underline{x}-\underline{x}'_i|^2}\right), \tag{5b}$$

$$F_{-\perp}^{(1)} = \frac{g}{2\pi}\sum_{j=1}^{A_2} T^a(\tilde{T}_j^a)\left(\,\delta(x_+ - y_{+j})\frac{\underline{x}-\underline{y}_j}{|\underline{x}-\underline{y}_j|^2} - \delta(x_+ - y'_{+j})\frac{\underline{x}-\underline{y}'_j}{|\underline{x}-\underline{y}'_j|^2}\right), \tag{5c}$$

$$F_{ij}^{(1)} = 0, \quad i,j = x,y. \tag{5d}$$

We note that the field strength is zero in the forward light cone. This is of course reasonable, because to order g there are no interactions between the pointlike charges constituting the nuclei. Therefore, no real gluons are produced.

III. GLUON FIELD TO NEXT-TO-LOWEST ORDER

A. Formal solution of the equations of motion

In this section we compute the solution of the Yang-Mills equations to order g^3. As we shall see, the equations of motion (2) are linear to each order, and we therefore focus first, for the sake of simplicity, on the case of a collision of two *single* pointlike color charges, for instance the quark from nucleon i in nucleus 1 and the quark from nucleon j in nucleus 2. The generalization to the nuclear collision is then straightforward: The solution is a simple superposition of the solutions emerging from each individual collision (i.e., a sum over i and j and over the respective quark-quark, quark-antiquark, antiquark-quark, and antiquark-antiquark scatterings).

To order g^3 the equations of motion (2) read

$$\Box A_\mu^{(3)} = J_\mu^{(3)} + ig[A^{(1)\nu}, \partial_\nu A_\mu^{(1)} + F_{\nu\mu}^{(1)}], \tag{6}$$

where $A_\mu^{(3)}$ and $J_\mu^{(3)}$ are the contributions to the gluon field and the fermionic current to order g^3. In order to solve these equations we have to first determine $J_\mu^{(3)}$. The most simple approach is to exploit (non-Abelian) current conservation $D_\mu J^\mu = 0$. One obtains,

$$\partial_\mu J^{(3)\mu} = ig[A_+^{(1)}, J_-^{(1)}] + ig[A_-^{(1)}, J_+^{(1)}] = \frac{g^3}{2\pi} f^{abc} T^a(T_i^b)(\tilde{T}_j^c)\,\delta(x_- - x_{-i})\,\delta(x_+ - y_{+j}) \times[\,\delta(\underline{x}-\underline{y}_j) - \delta(\underline{x}-\underline{x}_i)]\ln(|\underline{x}_i - \underline{y}_j|\lambda). \tag{7}$$

The charges are assumed to be recoilless and follow eikonal trajectories. Therefore, their momenta do not change in the interaction and the transverse component of the fermionic current is zero. The ''+'' and ''−'' components will still be δ functions on the light cone and in the transverse direction, as was the case at order g. The only effect of the collision on the valence charges is a ''rotation'' of their color, as soon as a charge ''hits'' the field of the other charge at the collision

point. This consideration leads us to the conclusion $J_+^{(3)} \sim \delta(x_- - x_{-i})\,\theta(x_+ - y_{+j})\,\delta(\underline{x} - \underline{x}_i)$ and $J_-^{(3)} \sim \theta(x_- - x_{-i})\,\delta(x_+ - y_{+j})\,\delta(\underline{x} - \underline{y}_j)$. The correct coefficients are found from Eq. (7):

$$J_+^{(3)} = -\frac{g^3}{2\pi} f^{abc} T^a (T_i^b)(\tilde{T}_j^c)\,\delta(x_- - x_{-i})\,\theta(x_+ - y_{+j}) \times \delta(\underline{x} - \underline{x}_i) \ln(|\underline{x}_i - \underline{y}_j|\lambda), \tag{8a}$$

$$J_-^{(3)} = \frac{g^3}{2\pi} f^{abc} T^a (T_i^b)(\tilde{T}_j^c)\,\theta(x_- - x_{-i})\,\delta(x_+ - y_{+j}) \times \delta(\underline{x} - \underline{y}_j) \ln(|\underline{x}_i - \underline{y}_j|\lambda), \tag{8b}$$

$$\underline{J}^{(3)} = 0. \tag{8c}$$

It can be shown that this current is consistent with the eikonal scattering limit of either the lowest order QCD diagrams for gluon radiation from two colliding color charges (cf. also Sec. III B below) or Wong's equations [15] for the collision of two classical color charges.

For one charge, say, i, ''hitting'' an ensemble of charges j, the color of charge i ''rotates'' each time it hits the field of one of the charges j in the ensemble. The resulting current is simply the sum over j of the terms on the right-hand side of Eq. (8). Similarly, the collision of an ensemble with an ensemble simply adds another summation over i. The actual nuclear collision in our approach is only slightly more complex in that one has to account for the presence of antiquarks as well.

The equations of motion for the next-to-lowest order gluon field are now obtained by inserting the lowest order results together with the current (8) into the right-hand side of Eq. (6):

$$\Box A_+^{(3)a} = \frac{g^3}{(2\pi)^2} f^{abc} (T_i^b)(\tilde{T}_j^c)[-2\pi \ln(|\underline{x}_i - \underline{y}_j|\lambda) \times \delta(x_- - x_{-i})\,\theta(x_+ - y_{+j})\,\delta(\underline{x} - \underline{x}_i) + \ln(|\underline{x} - \underline{x}_i|\lambda) \times \ln(|\underline{x} - \underline{y}_j|\lambda)\,\partial_+ \delta(x_- - x_{-i})\,\delta(x_+ - y_{+j})], \tag{9a}$$

$$\Box A_-^{(3)a} = \frac{g^3}{(2\pi)^2} f^{abc} (T_i^b)(\tilde{T}_j^c)[2\pi \ln(|\underline{x}_i - \underline{y}_j|\lambda)\,\theta(x_- - x_{-i}) \times \delta(x_+ - y_{+j})\,\delta(\underline{x} - \underline{y}_j) - \ln(|\underline{x} - \underline{x}_i|\lambda) \times \ln(|\underline{x} - \underline{y}_j|\lambda)\,\delta(x_- - x_{-i})\,\partial_- \delta(x_+ - y_{+j})], \tag{9b}$$

$$\Box \underline{A}^{(3)a} = \frac{g^3}{(2\pi)^2} f^{abc} (T_i^b)(\tilde{T}_j^c)\,\delta(x_- - x_{-i})\,\delta(x_+ - y_{+j}) \times \left(\ln(|\underline{x} - \underline{y}_j|\lambda)\,\frac{\underline{x} - \underline{x}_i}{|\underline{x} - \underline{x}_i|^2} - \ln(|\underline{x} - \underline{x}_i|\lambda)\,\frac{\underline{x} - \underline{y}_j}{|\underline{x} - \underline{y}_j|^2} \right). \tag{9c}$$

Equations (9) are linear differential equations, which justifies why we were able to focus on one single collision between two valence quarks first and later obtain the complete solution by summing over all possible collisions between color charges. (It was explained above how the corresponding sum over i and j and over quarks and antiquarks appears in the fermionic current; for the commutator term, its presence is obvious.) The linearity of Eqs. (9) also allows us to compute the solution simply by the method of Green functions. Since the classical solution obeys causality, we have to use the retarded Green function:

$$A_\mu^{(3)}(x) = \int d^4x'\, G_r(x - x')\,\tilde{J}_\mu(x'), \tag{10}$$

where $\tilde{J}_\mu \equiv J_\mu^{(3)} + ig[A^{(1)\nu}, \partial_\nu A_\mu^{(1)} + F_{\nu\mu}^{(1)}]$ is given explicitly by the right-hand side of Eq. (9). The retarded Green function reads, in coordinate and momentum space [16],

$$G_r(x) = \frac{1}{2\pi}\,\theta(t)\,\delta(x^2), \tilde{G}_r(k) = -\frac{1}{k^2 + i\epsilon k_0}. \tag{11}$$

Formulas (9)–(11) provide the classical gluon field to order g^3. Note that the above perturbative solution scheme renders the equations of motion linear at *each* successive order in g. In principle, one can therefore use the method of Green functions to construct the classical solution to arbitrary order in g. We shall argue below, however, that already at order g^5 quantum effects become important and the classical approach breaks down. Before we compute the solution to order g^3 explicitly, let us draw a connection to the perturbative solution via Feynman diagrams.

B. Connection to Feynman diagrams

Let us write the right-hand side of Eq. (10) in momentum representation,

$$A_\mu^{(3)a}(x) = -\int \frac{d^4k}{(2\pi)^4} \frac{e^{-ik\cdot x}}{k^2 + i\epsilon k_0} \tilde{J}_\mu^a(k), \tag{12}$$

where

$$\tilde{J}_+^a(k) = \frac{g^3}{(2\pi)^2} f^{abc} (T_i^b)(\tilde{T}_j^c) e^{i(k_+ x_{-i} + k_- y_{+j} - \underline{k}\cdot\underline{y}_j)} \times \int d^2\underline{q}\, e^{-i\underline{q}\cdot(\underline{x}_i - \underline{y}_j)} \frac{1}{(\underline{k} - \underline{q})^2} \left[\frac{i}{k_- + i\epsilon} - \frac{ik_+}{\underline{q}^2} \right], \tag{13a}$$

$$\tilde{J}_-^a(k) = -\frac{g^3}{(2\pi)^2} f^{abc} (T_i^b)(\tilde{T}_j^c) e^{i(k_+ x_{-i} + k_- y_{+j} - \underline{k}\cdot\underline{y}_j)} \times \int d^2\underline{q}\, e^{-i\underline{q}\cdot(\underline{x}_i - \underline{y}_j)} \frac{1}{\underline{q}^2} \left[\frac{i}{k_+ + i\epsilon} - \frac{ik_-}{(\underline{k} - \underline{q})^2} \right], \tag{13b}$$

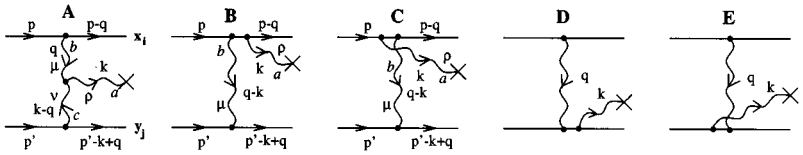

FIG. 2. Diagrams contributing to the gluon field at order g^3.

$$\underline{\tilde{J}}^a(k)=\frac{g^3}{(2\pi)^2}f^{abc}(T_i^b)(\tilde{T}_j^c)e^{i(k_+x_{-i}+k_-y_{+j}-\underline{k}\cdot\underline{y}_j)}$$

$$\times\int d^2\underline{q}\,e^{-i\underline{q}\cdot(\underline{x}_i-\underline{y}_j)}\frac{i(2\underline{q}-\underline{k})}{\underline{q}^2(\underline{k}-\underline{q})^2}. \tag{13c}$$

In order to derive this, we have made repeated use of

$$\int\frac{d^2\underline{q}}{(2\pi)^2}e^{i\underline{q}\cdot\underline{x}}\frac{1}{\underline{q}^2}=-\frac{1}{2\pi}\ln(|\underline{x}|\lambda) \tag{14}$$

and, for Eq. (13c), of the transverse gradient of this equation.

The diagrams giving the classical gluon field [11] at order g^3 are shown in Fig. 2. The cross at the end of the gluon line denotes the space-time point x where we measure the field. The upper quark line corresponds to the first charge (fixed coordinates $x_{-i},\underline{x}_i$), and the lower one corresponds to the second charge (at fixed $y_{+j},\underline{y}_j$). Therefore, the momentum on the upper line has a large ''+'' component, and the momentum on the lower line has a large ''−'' component. The gluon field to order g^3 also includes graphs where the two quarks do not interact. These diagrams are not shown in Fig. 2, since they are not part of the classical gluon field and do not contribute to gluon production (they vanish once we take the emitted gluon line to be on shell).

We take the gluon-fermion vertices in the eikonal approximation. In the standard calculation of the diagrams, the emitted gluon line corresponds to a gluon (Feynman) propagator $-i/(k^2+i\epsilon)$ times a phase $e^{-ik\cdot x}$ (since we shall ultimately transform the diagrams into coordinate space). This term is common to all diagrams in Fig. 2. However, as a result of the regularization of the Feynman propagator, all diagrams corresponding to gluon *absorption* (instead of emission) are automatically included in this calculation. That means that the usual Feynman diagrams yield an acausal result. In order to establish correspondence to the classical result, where there is only gluon emission, we replace the Feynman propagator by the *retarded* propagator $-i/(k^2+i\epsilon k_0)$ for the gluon field measured at x.

Similarly, as a result of the Feynman regularization of the fermion propagator, all diagrams B–E contain contributions where the gluon is emitted *prior* to the one-gluon exchange. To ensure causality, we have to use a *retarded* fermion propagator when calculating the diagrams B and D and an *advanced* fermion propagator in diagrams C and E which renders the emission of the gluon causal.

We have the freedom to change the regularization of propagators. Different choices of regularization do not influence the physics. The difference between the retarded (or advanced) propagators and the usual Feynman propagator is just a δ function of the square of the four-momentum of the internal line. Therefore, for graphs B–E this difference is proportional to those parts of the diagrams where the fermion line is on shell. But these parts do not contribute to real gluon production, since once we put the outgoing gluon on-shell, they vanish. The regularization of the internal gluon lines of the diagrams in Fig. 2 turns out to be of no importance for the actual calculation.

After clarifying the regularization of the propagators, we compute the diagrams according to the usual Feynman rules in covariant gauge. Let us denote the ρth component of the gluon field from a diagram X by $X|_\rho$, where $X=A$, B, C, D, or E. Diagram A is nonzero for all values of ρ, while for B and C only the ''+'' component and for D and E only the ''−'' component are nonvanishing. After a lengthy, but straightforward calculation we compare with Eqs. (12) and (13) to obtain the identities

$$A_+^{(3)a}(x)=(A+B+C)|_{\rho=+}, \tag{15a}$$

$$A_-^{(3)a}(x)=(A+D+E)|_{\rho=-}, \tag{15b}$$

$$\underline{A}^{(3)a}(x)=A|_{\rho=\perp}. \tag{15c}$$

We see that the calculation of the diagrams yields exactly the gluon field (12) obtained from the classical solution of the Yang-Mills equations. That proves the correspondence of the classical field to the diagrams in Fig. 2. The diagram A arises from the commutator term on the right-hand side of Eq. (6), whereas graphs B–E arise from the fermionic current.

The order g^3 is the limit of applicability of the classical approach to the problem of gluon production. At order g^5 one can construct diagrams which contribute to gluon production, but cannot be obtained classically. An example of this type is shown in Fig. 3.

The two-gluon exchange contribution (Fig. 3) calculated using the traditional Feynman regularization of the propagators cannot be obtained from the classical equations of motion. The classical approach would give the part of the diagram where the two exchanged gluons are in a color singlet state. That corresponds to the internal fermion lines between the exchanged gluons being on shell. This is what one would obtain by iterating the procedure for the determination of the classical field outlined above to higher orders in the coupling. The color octet combination of the two gluons, being

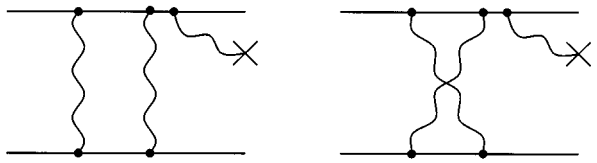

FIG. 3. Graphs contributing to the gluon production at order g^5.

the lowest order correction to the gluon's Regge trajectory, is a pure ''quantum'' effect. A different regularization of the propagators cannot make this contribution ''classical.'' One can see that by a direct calculation of the two-gluon exchange diagrams in the octet channel. The resulting contribution is proportional to $\ln s$, where s is the center-of-mass energy of the colliding quarks (see [17] and references mentioned there). That is, it depends on the longitudinal momenta of the quarks. However, the classical calculation is just an iteration of the one-gluon exchange diagram and thus not able to provide such a logarithmic longitudinal dependence. Therefore, the diagrams in Fig. 3 are not classical. (After all, it would be quite surprising if the gluon's Regge trajectory turns out to be a classical concept.)

C. Classical gluon field in coordinate space

Let us now explicitly compute the gluon field (10) in coordinate space. We decompose the ''+'' component of the field as

$$A_+^{(3)a}=a_1+a_2, \tag{16}$$

where a_1 is straightforwardly computed:

$$\begin{aligned} a_1 &= -\frac{g^3}{2\pi} f^{abc}(T_i^b)(\tilde{T}_j^c)\int d^4x' G_r(x-x')\ln(|\underline{x}_i-\underline{y}_j|\lambda)\,\delta(x'_- - x_{-i})\,\theta(x'_+ - y_{+j})\,\delta(\underline{x}'-\underline{x}_i) \\ &= -\frac{g^3}{2(2\pi)^2} f^{abc}(T_i^b)(\tilde{T}_j^c)\frac{1}{x_- - x_{-i}}\,\theta(x_- - x_{-i})\,\theta\left(x_+ - y_{+j} - \frac{|\underline{x}-\underline{x}_i|^2}{2(x_- - x_{-i})}\right)\ln(|\underline{x}_i-\underline{y}_j|\lambda). \end{aligned} \tag{17}$$

The second term can be written in the form

$$\begin{aligned} a_2 &= \frac{g^3}{(2\pi)^2} f^{abc}(T_i^b)(\tilde{T}_j^c)\int d^4x' G_r(x-x')\ln(|\underline{x}'-\underline{x}_i|\lambda)\ln(|\underline{x}'-\underline{y}_j|\lambda)\,\partial'_+\,\delta(x'_- - x_{-i})\,\delta(x'_+ - y_{+j}) \\ &= \frac{g^3}{2(2\pi)^2} f^{abc}(T_i^b)(\tilde{T}_j^c)\partial_+[\,\theta(x_- - x_{-i})\,\theta(x_+ - y_{+j})\mathcal{J}], \end{aligned} \tag{18}$$

with

$$\mathcal{J}\equiv\int \frac{d^2\underline{q}\,d^2\underline{l}}{(2\pi)^2} e^{-i\underline{q}\cdot(\underline{x}-\underline{y}_j)-i\underline{l}\cdot(\underline{x}-\underline{x}_i)}\frac{1}{\underline{l}^2\underline{q}^2} J_0(|\underline{q}+\underline{l}|\tau), \tag{19}$$

where $\tau=\sqrt{2(x_- - x_{-i})(x_+ - y_{+j})}$. The explicit evaluation of the integral $\mathcal{J}$ is referred to Appendix A. The final result is

$$\mathcal{J}=\ln(\xi_>\lambda)\ln(\eta_>\lambda)+\frac{1}{4}\left[\mathrm{Li}_2\left(e^{i\alpha}\frac{\xi_<\eta_<}{\xi_>\eta_>}\right)+\mathrm{Li}_2\left(e^{-i\alpha}\frac{\xi_<\eta_<}{\xi_>\eta_>}\right)\right], \tag{20}$$

where $\xi_{>(<)}=\max(\min)(|\underline{x}-\underline{x}_i|,\tau)$, $\eta_{>(<)}=\max(\min)(|\underline{x}-\underline{y}_j|,\tau)$, and α is the angle between $\underline{x}-\underline{x}_i$ and $\underline{x}-\underline{y}_j$. λ plays the same role as in Eq. (4). $\mathrm{Li}_2(z)$ is the dilogarithm (also known as Spence's function). With the final expression for a_2 we obtain

$$\begin{aligned} A_+^{(3)a}(x) = -\frac{g^3}{2(2\pi)^2} f^{abc}(T_i^b)(\tilde{T}_j^c)\Bigg[& \frac{1}{x_- - x_{-i}}\,\theta(x_- - x_{-i})\,\theta\left(x_+ - y_{+j} - \frac{|\underline{x}-\underline{x}_i|^2}{2(x_- - x_{-i})}\right)\ln(|\underline{x}_i-\underline{y}_j|\lambda) \\ & - \delta(x_- - x_{-i})\,\theta(x_+ - y_{+j})\ln(|\underline{x}-\underline{x}_i|\lambda)\ln(|\underline{x}-\underline{y}_j|\lambda) - \theta(x_- - x_{-i})\,\theta(x_+ - y_{+j})\partial_+[\ln(\xi_>\lambda)\ln(\eta_>\lambda)] \\ & + \frac{1}{4}\,\theta(x_- - x_{-i})\,\theta(x_+ - y_{+j})(\partial_+ \ln r)\ln(1-2r\cos\alpha+r^2)\Bigg], \end{aligned} \tag{21}$$

where $r=(\xi_<\eta_<)/(\xi_>\eta_>)$.

The integrations for $A_-^{(3)a}$ are done similarly with the result

$$\begin{aligned} A_-^{(3)a}(x) = \frac{g^3}{2(2\pi)^2} f^{abc}(T_i^b)(\tilde{T}_j^c)\Bigg[& \frac{1}{x_+ - y_{+j}}\,\theta(x_+ - y_{+j})\,\theta\left(x_- - x_{-i} - \frac{|\underline{x}-\underline{y}_j|^2}{2(x_+ - y_{+j})}\right)\ln(|\underline{x}_i-\underline{y}_j|\lambda) \\ & - \delta(x_+ - y_{+j})\,\theta(x_- - x_{-i})\ln(|\underline{x}-\underline{x}_i|\lambda)\ln(|\underline{x}-\underline{y}_j|\lambda) - \theta(x_- - x_{-i})\,\theta(x_+ - y_{+j})\partial_-[\ln(\xi_>\lambda)\ln(\eta_>\lambda)] \\ & + \frac{1}{4}\,\theta(x_- - x_{-i})\,\theta(x_+ - y_{+j})(\partial_- \ln r)\ln(1-2r\cos\alpha+r^2)\Bigg]. \end{aligned} \tag{22}$$

For $\underline{A}^{(3)a}$ we find

$$\underline{A}^{(3)a}(x) = -\frac{g^3}{2(2\pi)^2} f^{abc}(T_i^b)(\widetilde{T}_j^c)\,\theta(x_- - x_{-i})\,\theta(x_+ - y_{+j})[(\nabla_i - \nabla_j)\mathcal{J}]$$

$$= -\frac{g^3}{2(2\pi)^2} f^{abc}(T_i^b)(\widetilde{T}_j^c)\,\theta(x_- - x_{-i})\,\theta(x_+ - y_{+j})\Bigg[(\nabla_i - \nabla_j)[\ln(\xi_>\lambda)\ln(\eta_>\lambda)] - \frac{1}{4}[(\nabla_i - \nabla_j)\ln r]$$

$$\times \ln(1 - 2r\cos\alpha + r^2) - \frac{i}{4}[(\nabla_i - \nabla_j)\alpha]\ln\left(\frac{1 - re^{i\alpha}}{1 - re^{-i\alpha}}\right)\Bigg]. \tag{23}$$

As expected, the solution to order g^3 is causal; i.e., it is nonvanishing *only* in the forward light cone.

To obtain the complete solution for the nucleus-nucleus collision we simply sum over all charges in the nuclei; i.e., as discussed above, we sum over all nucleons i and j and over quarks and antiquarks inside the nucleons. If we denote the solution of the scattering problem of two single charges with coordinates x_i and y_j found above by $A_\mu^{(3)a}(x, x_i, y_j)$, we obtain

$$A_\mu^{(3)a}(x) = \sum_{i,j=1}^{A_1, A_2} [A_\mu^{(3)a}(x, x_i, y_j) - A_\mu^{(3)a}(x, x_i', y_j) - A_\mu^{(3)a}(x, x_i, y_j') + A_\mu^{(3)a}(x, x_i', y_j')]. \tag{24}$$

The antiquark coordinates are marked with a prime. The relative signs emerge from the fact that antiquarks have the same color charge as quarks, but with opposite sign.

IV. RADIATED FIELD ENERGY, NUMBER, AND MULTIPLICITY DISTRIBUTIONS

In order to determine the radiated field energy we start from Eq. (12), and, for simplicity, discuss the case of a single collision first. Note that a part of the solution corresponds just to a change of the field carried by the charge due to the collision (the color ''rotation''), and not to the radiated gluon field. That part is most easily isolated by a contour integration in the complex k_0 plane in Eq. (12); it arises from the pole $k_\pm = -i\epsilon$ in Eq. (13):

$$\underline{A}^{(3)a}_{+\,\mathrm{charge}}(x) = \frac{g^3}{(2\pi)^2} f^{abc}(T_i^b)(\widetilde{T}_j^c)\ln(|\underline{x}_i - \underline{y}_j|\lambda) \times \ln(|\underline{x} - \underline{x}_i|\lambda)\,\delta(x_- - x_{-i})\,\theta(x_+ - y_{+j}), \tag{25a}$$

$$\underline{A}^{(3)a}_{-\,\mathrm{charge}}(x) = -\frac{g^3}{(2\pi)^2} f^{abc}(T_i^b)(\widetilde{T}_j^c)\ln(|\underline{x}_i - \underline{y}_j|\lambda) \times \ln(|\underline{x} - \underline{y}_j|\lambda)\,\theta(x_- - x_{-i})\,\delta(x_+ - y_{+j}), \tag{25b}$$

$$\underline{A}^{(3)a}_{\mathrm{charge}}(x) = 0. \tag{25c}$$

The radiated gluon field arises from the poles of the retarded propagator in Eq. (12); i.e., it corresponds to on-shell gluons, as one would expect:

$$A^{(3)a}_{\mu\,\mathrm{rad}}(x) = \theta(t - t_{ij}) \int d\widetilde{k}[i\widetilde{J}^a_\mu(\omega, \mathbf{k})e^{-i\omega t + i\mathbf{k}\cdot\mathbf{x}} + \text{c.c.}], \tag{26}$$

where $t_{ij} \equiv (x_{-i} + y_{+j})/\sqrt{2}$ is the time when the collision happens and $d\widetilde{k} \equiv d^3\mathbf{k}/[(2\pi)^3 2\omega]$, with $\omega = |\mathbf{k}|$ [16]. Obviously, this field vanishes prior to the collision.

The (stationary part of the) radiated field energy is [16]

$$\mathcal{H} = \int d\widetilde{k}\,\omega[\underline{\widetilde{J}}^a(\omega, \mathbf{k}) \cdot \underline{\widetilde{J}}^{a*}(\omega, \mathbf{k}) - \widetilde{J}^a_+(\omega, \mathbf{k})\widetilde{J}^{a*}_-(\omega, \mathbf{k}) - \widetilde{J}^a_-(\omega, \mathbf{k})\widetilde{J}^{a*}_+(\omega, \mathbf{k})]. \tag{27}$$

In the case of a nuclear collision $\widetilde{J}^a_\mu(k)$, Eq. (13), becomes more complicated: There is an additional sum over nucleons i and j and over quarks and antiquarks inside these nucleons. Inserting the resulting expression, for times *after* the *last* parton-parton collision we arrive at

$$\mathcal{H} = 4\frac{g^6}{(2\pi)^4} f^{abc} f^{ade} \int d\widetilde{k}\,\omega \frac{1}{\underline{k}^2} \times \int d^2\underline{q}_1 d^2\underline{q}_2 \frac{\underline{q}_1 \cdot \underline{q}_2 \underline{k}^2 + \underline{q}_1^2 \underline{q}_2^2 - \underline{q}_1^2 \underline{k} \cdot \underline{q}_2 - \underline{q}_2^2 \underline{k} \cdot \underline{q}_1}{\underline{q}_1^2 \underline{q}_2^2 (\underline{k} - \underline{q}_1)^2 (\underline{k} - \underline{q}_2)^2} \times \sum_{i,k=1}^{A_1} \sum_{j,l=1}^{A_2} (T_i^b)(\widetilde{T}_j^c)(T_k^d)(\widetilde{T}_l^e)\mathcal{P}(k_+, \underline{q}_1; x_i)\,\mathcal{P}(k_-, \underline{k} - \underline{q}_1; y_j)\mathcal{P}^*(k_+, \underline{q}_2; x_k)\mathcal{P}^*(k_-, \underline{k} - \underline{q}_2; y_l), \tag{28}$$

where now $k_\pm \equiv (\omega \pm k^z)/\sqrt{2}$ and

$$\mathcal{P}(k_+, \underline{q}; x_i) \equiv e^{ik_+ x_{-i} - i\underline{q}\cdot\underline{x}_i} - e^{ik_+ x'_{-i} - i\underline{q}\cdot\underline{x}'_i}. \tag{29}$$

In order to achieve color neutrality in the initial state, we have to average over all possible color orientations in the color space of the individual nucleons. With $\mathrm{tr}[(T_i^b)(\widetilde{T}_j^c)(T_k^d)(\widetilde{T}_l^e)] = \delta_{ik}\delta^{bd}\delta_{jl}\delta^{ce}/4$, and $f^{abc}f^{abc} = N_c(N_c^2 - 1)$ this yields

$$\frac{1}{N_c^2}\mathrm{tr}[\mathcal{H}]=\frac{g^6}{(2\pi)^4}\frac{N_c^2-1}{N_c}\int d\tilde{k}\frac{\omega}{\underline{k}^2}\int d^2\underline{q}_1 d^2\underline{q}_2 \times\frac{\underline{q}_1\cdot\underline{q}_2\underline{k}^2+\underline{q}_1^2\underline{q}_2^2-\underline{q}_1^2\underline{k}\cdot\underline{q}_2-\underline{q}_2^2\underline{k}\cdot\underline{q}_1}{\underline{q}_1^2\underline{q}_2^2(\underline{k}-\underline{q}_1)^2(\underline{k}-\underline{q}_2)^2}\widetilde{\mathcal{P}}(k,\underline{q}_1,\underline{q}_2), \tag{30}$$

where

$$\widetilde{\mathcal{P}}(k,\underline{q}_1,\underline{q}_2)\equiv\sum_{i=1}^{A_1}\mathcal{P}(k_+,\underline{q}_1;x_i)\mathcal{P}^*(k_+,\underline{q}_2;x_i) \times\sum_{j=1}^{A_2}\mathcal{P}(k_-,\underline{k}-\underline{q}_1;y_j)\mathcal{P}^*(k_-,\underline{k}-\underline{q}_2;y_j). \tag{31}$$

For further evaluation we introduce the center-of-mass coordinates of nucleon $i,(X_{-i},\underline{X}_i)$, and nucleon $j,(Y_{+j},\underline{Y}_j)$, and relative coordinates $\Delta x_{-i},\Delta\underline{x}_i,\Delta y_{+j},\Delta\underline{y}_j$, such that

$$x_{-i}=X_{-i}+\frac{\Delta x_{-i}}{2},\quad x'_{-i}=X_{-i}-\frac{\Delta x_{-i}}{2},$$

$$y_{+j}=Y_{+j}+\frac{\Delta y_{+j}}{2},\quad y'_{+j}=Y_{+j}-\frac{\Delta y_{+j}}{2}, \tag{32a}$$

$$\underline{x}_i=\underline{X}_i+\frac{\Delta\underline{x}_i}{2},\quad \underline{x}'_i=\underline{X}_i-\frac{\Delta\underline{x}_i}{2},$$

$$\underline{y}_j=\underline{Y}_j+\frac{\Delta\underline{y}_j}{2},\quad \underline{y}'_j=\underline{Y}_j-\frac{\Delta\underline{y}_j}{2}. \tag{32b}$$

Here we assumed that the positions of quark and antiquark in a nucleon are symmetric with respect to the center of the nucleon. This assumption is not crucial. The calculations can also be done for the general case of arbitrary positions of quarks and antiquarks in the nucleons. For the ''symmetric'' case the phase factor becomes

$$\widetilde{\mathcal{P}}(k,\underline{q}_1,\underline{q}_2)=\sum_{i=1}^{A_1}e^{-i(\underline{q}_1-\underline{q}_2)\cdot\underline{X}_i}[e^{-i(\underline{q}_1-\underline{q}_2)\cdot\Delta\underline{x}_i/2} -e^{ik_+\Delta x_{-i}-i(\underline{q}_1+\underline{q}_2)\cdot\Delta\underline{x}_i/2}+\mathrm{c.c.}] \times\sum_{j=1}^{A_2}e^{i(\underline{q}_1-\underline{q}_2)\cdot\underline{Y}_j}[e^{i(\underline{q}_1-\underline{q}_2)\cdot\Delta\underline{y}_j/2} -e^{ik_-\Delta y_{+j}-i\underline{k}\cdot\Delta\underline{y}_j+i(\underline{q}_1+\underline{q}_2)\cdot\Delta\underline{y}_j/2}+\mathrm{c.c.}]. \tag{33}$$

We shall now first average $\widetilde{\mathcal{P}}$ over the longitudinal positions of quarks and antiquarks inside the nucleons. The nuclei are highly Lorentz contracted in the longitudinal direction. To simplify the subsequent discussion, we take them and the nucleons inside to be cylindrical. Each nucleon is then a cylinder of radius a and length $2a/\gamma$, oriented along the z axis, where γ is the Lorentz factor in the c.m. frame of the collision. (The longitudinal extension of the nucleons is not important; it will drop out in the following anyway.) With

$$\frac{\gamma}{\sqrt{2}a}\int_{-a/\sqrt{2}\gamma}^{a/\sqrt{2}\gamma}d\left(\frac{\Delta x_{-i}}{2}\right)e^{ik_+\Delta x_{-i}}=\frac{\sin[k_+\sqrt{2}a/\gamma]}{k_+\sqrt{2}a/\gamma}\to 1\,(\gamma\to\infty), \tag{34}$$

and an analogous relation for the average over Δy_{+j}, the longitudinal momentum dependence vanishes from the phase factor.

Let us now average over the transverse positions $\underline{X}_i,\underline{Y}_j$ of the nucleons inside a nuclear transverse area. For a cylindrical nucleus, the transverse area which we average over is independent of the longitudinal position of the individual nucleon and equal to $\pi R_{1(2)}^2$, $R_{1(2)}$ being the transverse radius of nucleus 1 (2). Let us take nucleus 1 to be the larger of the two nuclei. Since R_1 is by far larger than the (inverse) momentum scales we are interested in, we may take to good approximation $R_1\to\infty$, and obtain

$$\frac{1}{\pi R_1^2}\int d^2\underline{X}_i e^{-i(\underline{q}_1-\underline{q}_2)\cdot\underline{X}_i}\simeq\frac{4\pi}{R_1^2}\delta(\underline{q}_1-\underline{q}_2). \tag{35}$$

With this result, the $\underline{Y}_j$ average (over the transverse positions of nucleons in nucleus 2) is trivial. The assumption of infinite transverse nuclear size greatly simplifies the subsequent discussion. However, we are then no longer able to study collisions at finite impact parameter.

Finally, we average over the transverse dimension of the nucleons. That integral is formally the same as Eq. (35), only that R_1 is replaced by a and the momentum dependences of the various terms in $\widetilde{\mathcal{P}}$ are different. Now, however, $1/a$ is not small on the momentum scale of interest. In fact, the $\underline{q}_{1,2}$ integrations in Eq. (30) are logarithmically divergent, such that the treatment of the small momentum region is of some importance. As we shall see, treating the average over the transverse dimensions of the nucleons correctly leads to an infrared regularization of these divergences via nucleonic form factors. The physical interpretation is that on large (spatial) scales individual nucleons appear colorless and do not emit gluons.

The average over the transverse dimension of a nucleon involves typically integrals of the type [18]

$$\frac{1}{\pi a^2}\int d^2\left(\frac{\Delta\underline{x}_i}{2}\right)e^{i\underline{q}\cdot\Delta\underline{x}_i/2}=\frac{2J_1(|\underline{q}|a)}{|\underline{q}|a}. \tag{36}$$

For the average phase factor we thus obtain

$$\langle\widetilde{\mathcal{P}}(k,\underline{q}_1,\underline{q}_2)\rangle=4A_1A_2\frac{4\pi}{R_1^2}\delta(\underline{q}_1-\underline{q}_2)\left(1-\frac{2J_1(2|\underline{q}_1|a)}{2|\underline{q}_1|a}\right) \times\left(1-\frac{2J_1(2|\underline{k}-\underline{q}_1|a)}{2|\underline{k}-\underline{q}_1|a}\right). \tag{37}$$

Our final result for the invariant distribution of the average energy is

$$\frac{d\langle\mathcal{H}\rangle}{dyd^2\underline{k}}=\pi\frac{g^6}{(2\pi)^6}\frac{N_c^2-1}{N_c}\frac{4A_1A_2}{\pi R_1^2}\frac{\omega}{\underline{k}^2}\times\int d^2\underline{q}\frac{F(|\underline{q}|a)}{\underline{q}^2}\frac{F(|\underline{k}-\underline{q}|a)}{(\underline{k}-\underline{q})^2},\tag{38}$$

with the (longitudinal) gluon rapidity $y\equiv\ln[k_+/k_-]/2$ and the ''form factor'' $F(x)=1-2J_1(2x)/2x$. For small $\underline{q}$ or $\underline{k}-\underline{q}$, F regularizes the infrared divergence of the integral. If we do not assume that the quark and antiquark are symmetric with respect to the nucleon's center and allow them to be anywhere in the nucleon, the ''form factor'' becomes $F(x)=1-[2J_1(x)/x]^2$.

We now compare our result to that of [9]. In that work, the *number distribution* of radiated gluons was related to the average energy distribution via

$$\frac{d\mathcal{N}}{dyd^2\underline{k}}\equiv\frac{1}{\omega}\frac{d\langle\mathcal{H}\rangle}{dyd^2\underline{k}}.\tag{39}$$

As in [9], we consider a central collision of equal nuclei, $A_1=A_2=A$. According to [11], the average transverse color charge density is given by $\mu^2=C_FA/(N_c\pi R^2)$ (for our case of a ''cylindrical'' nucleus), where $C_F\equiv(N_c^2-1)/(2N_c)$. Then, with the transverse area $S_\perp\equiv\pi R^2$,

$$\frac{d\mathcal{N}}{dyd^2\underline{k}}=S_\perp\frac{\pi}{C_F^2}\frac{2g^6\mu^4}{(2\pi)^3\pi}N_c(N_c^2-1)\frac{1}{\underline{k}^2}\times\int\frac{d^2\underline{q}}{(2\pi)^2}\frac{F(|\underline{q}|a)}{\underline{q}^2}\frac{F(|\underline{k}-\underline{q}|a)}{(\underline{k}-\underline{q})^2}.\tag{40}$$

This has (apart from the form factors) the same momentum dependence as the result of [9] [Eq. (49)]. The prefactor, though different from [9], agrees with recent results obtained by Gyulassy and McLerran [19]. Note that as a result of the form factors, our result behaves like $1/\underline{k}^2$ for small $|\underline{k}|\sim1/a$. The residual infrared divergence stems from our approximation of an infinitely large nucleus in Eq. (35). This divergence is actually cut off by the finite (inverse) size of the nucleus (i.e., by the nuclear form factor). In this range of momenta, however, our treatment ceases to be valid anyway, since then $|\underline{k}|\sim1/R\ll1/a\sim\Lambda_{\rm QCD}$, while one of our initial assumptions was $|\underline{k}|\gg\Lambda_{\rm QCD}$.

The gluon *number* distribution (40) is *not* directly accessible in the experiment. Experimentally, one measures the (invariant) differential cross section for detecting a radiated gluon, $d\sigma_{\rm rad}/dyd^2\underline{k}$, divided by the total cross section of the collision. Equivalently, one can divide the gluon *number* distribution (40) by the total number of scattering events with one-gluon exchange between the color charges in a (central) $A+A$ collision. This number can be obtained quite analogously to the above derivation of the number distribution for radiated gluons. Instead of Eq. (28) we start with the square of the one-gluon exchange amplitude. This amplitude for two charges (whose coordinates are specified as in Sec. III) is

$$-\frac{ig^2}{(2\pi)^2}(T_i^a)(\tilde{T}_j^a)\int\frac{d^2\underline{q}}{\underline{q}^2}e^{i\underline{q}\cdot(\underline{y}_j-\underline{x}_i)}.\tag{41}$$

Similar to the above, after averaging the modulus squared of this amplitude over the positions of the quarks and antiquarks inside the nucleons and nucleons in the nucleus, as well as over quark colors in the initial state, we obtain

$$\mathcal{N}_{\rm tot}=4\alpha_S^2\frac{C_F}{2N_c}\frac{4A^2}{\pi R^2}\int d^2\underline{q}\left(\frac{F(|\underline{q}|a)}{\underline{q}^2}\right)^2.\tag{42}$$

The final answer for the gluon *multiplicity* distribution is

$$\frac{dn}{dyd^2\underline{k}}=\frac{1}{\mathcal{N}_{\rm tot}}\frac{d\mathcal{N}}{dyd^2\underline{k}}=\frac{N_c\alpha_S}{\pi^2\underline{k}^2}\int d^2\underline{q}\frac{F(|\underline{q}|a)}{\underline{q}^2}\frac{F(|\underline{k}-\underline{q}|a)}{(\underline{k}-\underline{q})^2}\times\left[\int d^2\underline{q}\left(\frac{F(|\underline{q}|a)}{\underline{q}^2}\right)^2\right]^{-1}.\tag{43}$$

Expanding the form factor (in the ''symmetric'' case) for small a, $F(x)\simeq x^2/(2+x^2/3)$ for $x\to0$, and choosing $m_\rho^2\equiv24/a^2$, this result coincides with that of [14] [Eq. (21)], since $C_A\equiv N_c=3$.

For the case of a nucleon in which the positions of quark and antiquark are symmetric with respect to its center one can explicitly perform the integration in Eq. (43). The result reads

$$\frac{dn}{dyd^2\underline{k}}=\frac{N_c\alpha_S}{\pi^2\underline{k}^2}\frac{12}{5}\left(-\frac{1+(\underline{k}a)^2}{(\underline{k}a)^4}[1-J_0(2|\underline{k}|a)]+\frac{2+(\underline{k}a)^2}{(\underline{k}a)^4}J_2(2|\underline{k}|a)+{}_2F_3(1,1;2,2,2;-\underline{k}^2a^2)\right).\tag{44}$$

The details of the integration are given in Appendix B. For $\underline{k}\to0$, the expression in large parentheses becomes 5/12, as expected from Eq. (43).

V. CONCLUSIONS

In this paper we have solved the classical Yang-Mills equations for a collision of ultrarelativistic nuclei. Our solution assumes the nuclei to have the form used in [11] and the color charges to follow eikonal trajectories during the collision. The solution is constructed perturbatively in covariant (Lorentz) gauge to lowest order (Abelian limit, order g) and next-to-lowest order (g^3). Via Feynman diagrams we have clarified the connection between the classical and quantum solution to order g^3.

We have established a limit for the classical description of gluon production. From the discussion of the diagrams in Sec. III B follows that the limit for the field is one gluon per nucleon, unless the second gluon is the outgoing gluon. That means that in the diagrammatic formulation of the problem there should be no more than one gluon leaving each nucleon. In nuclear collisions, different from the case of a

single nucleus [12], we cannot require the final states of the nucleons to be color singlets. Therefore, here we cannot apply color averaging which cancels quantum corrections (as described in [12]) and puts internal fermion lines of graphs like in Fig. 3 on shell, allowing for a classical description. That way the limit of the classical approach is reduced to one gluon per nucleon.

We have given explicit expressions for the gluon field in coordinate space [Eqs. (21)–(23)] and calculated the energy, number, and multiplicity distributions of radiated gluons to order g^3 [Eqs. (38), (40), and (43)]. Our result for the number distribution agrees with [19] and the form factors of the individual nucleons can be cast into a form such that the multiplicity distribution agrees with the result of [14].

The resulting gluon number and multiplicity distributions are boost invariant, a property which was *a priori* assumed in [9]. Boost invariance is also assumed in popular hydrodynamic models [20] to describe the evolution of ultrarelativistic nuclear collisions after (local) thermalization is established. To answer the question whether thermalization actually happens and what the respective time scales are, it is planned to utilize the solution found here to study screening and damping in the radiation-produced gluonic medium [21].

ACKNOWLEDGMENTS

The authors would like to thank S. Brodsky, M. Gyulassy, A.H. Mueller, B. Müller, S. Pratt, R. Venugopalan, and J. Verbaarschot for interesting discussions and helpful advice. The research of Yu.V.K. was sponsored in part by the U.S. Department of Energy under Grant No. DE-FG02-94ER-40819. The work of D.H.R. was supported in part by the U.S. Department of Energy under Contract No. DE-FG02-96ER-40945.

APPENDIX A

In this appendix we explicitly calculate the integral

$$\mathcal{J}=\int \frac{d^2\underline{q}\,d^2\underline{l}}{(2\pi)^2}\,\frac{e^{-i\underline{q}\cdot(\underline{x}-\underline{y}_j)-i\underline{l}\cdot(\underline{x}-\underline{x}_i)}}{\underline{l}^2\underline{q}^2}J_0(|\underline{q}+\underline{l}|\tau). \quad \text{(A1)}$$

Using the addition theorem for Bessel functions (ϕ is the angle between $\underline{q}$ and $\underline{l}$),

$$J_0(|\underline{q}+\underline{l}|\tau)=\sum_{k=-\infty}^{\infty}(-1)^k e^{ik\phi}J_k(|\underline{q}|\tau)J_k(|\underline{l}|\tau), \quad \text{(A2)}$$

we obtain

$$\mathcal{J}=\sum_{k=-\infty}^{\infty}(-1)^k\int \frac{d^2\underline{q}\,d^2\underline{l}}{(2\pi)^2}\,\frac{e^{-i\underline{q}\cdot(\underline{x}-\underline{y}_j)-i\underline{l}\cdot(\underline{x}-\underline{x}_i)}}{\underline{l}^2\underline{q}^2} \times e^{ik\phi}J_k(|\underline{q}|\tau)J_k(|\underline{l}|\tau). \quad \text{(A3)}$$

If ϕ_1 is the angle between $\underline{l}$ and $\underline{x}-\underline{x}_i$ and ϕ_2 is the angle between $\underline{q}$ and $\underline{x}-\underline{y}_j$, we can express ϕ as

$$\phi=\phi_2-\phi_1+\alpha, \quad \text{(A4)}$$

with α being the angle between $\underline{x}-\underline{y}_j$ and $\underline{x}-\underline{x}_i$. All angles are taken clockwise. Integrating over ϕ_1 and ϕ_2 we obtain,

$$\mathcal{J}=\sum_{k=-\infty}^{\infty}e^{ik\alpha}\left(\int_0^\infty\frac{dq}{q}J_k(q|\underline{x}-\underline{y}_j|)J_k(q\tau)\right) \times\left(\int_0^\infty\frac{dl}{l}J_k(l|\underline{x}-\underline{x}_i|)J_k(l\tau)\right). \quad \text{(A5)}$$

For nonzero k we can use the formula (see [22])

$$\int_0^\infty\frac{dl}{l}J_k(l|\underline{x}-\underline{x}_i|)J_k(l\tau)=\frac{1}{2k}\left(\frac{\xi_<}{\xi_>}\right)^k, \quad k>0, \quad \text{(A6)}$$

where $\xi_{>(<)}=\max(\min)(|\underline{x}-\underline{x}_i|,\tau)$, to obtain the series

$$\sum_{k=1}^{\infty}(e^{ik\alpha}+e^{-ik\alpha})\frac{1}{4k^2}\left(\frac{\xi_<\eta_<}{\xi_>\eta_>}\right)^k, \quad \text{(A7)}$$

with $\eta_{>(<)}=\max(\min)(|\underline{x}-\underline{y}_j|,\tau)$. Using the definition of the dilogarithm,

$$\mathrm{Li}_2(z)\equiv\sum_{k=1}^{\infty}\frac{z^k}{k^2}, \quad \text{(A8)}$$

we can rewrite this series as

$$\frac{1}{4}\left[\mathrm{Li}_2\left(e^{i\alpha}\frac{\xi_<\eta_<}{\xi_>\eta_>}\right)+\mathrm{Li}_2\left(e^{-i\alpha}\frac{\xi_<\eta_<}{\xi_>\eta_>}\right)\right]. \quad \text{(A9)}$$

For the $(k=0)$ term in Eq. (A5) one can show that since

$$\int_\mu^\infty\frac{dl}{l}J_0(l|\underline{x}-\underline{x}_i|)J_0(l\tau)=-\ln\left(\frac{\xi_>\mu}{2}\right)-\gamma, \quad \text{(A10)}$$

with γ being the Euler constant, this term can be rewritten as

$$\ln(\xi_>\lambda)\ln(\eta_>\lambda), \quad \text{(A11)}$$

where the cutoff λ includes the previous cutoff μ and all other numerical prefactors. We finally obtain the answer,

$$\mathcal{J}=\ln(\xi_>\lambda)\ln(\eta_>\lambda)+\frac{1}{4}\left[\mathrm{Li}_2\left(e^{i\alpha}\frac{\xi_<\eta_<}{\xi_>\eta_>}\right) +\mathrm{Li}_2\left(e^{-i\alpha}\frac{\xi_<\eta_<}{\xi_>\eta_>}\right)\right]. \quad \text{(A12)}$$

APPENDIX B

The goal of this appendix is to perform the integration

$$\mathcal{I}=\int\frac{d^2\underline{q}}{\underline{q}^2(\underline{k}-\underline{q})^2}\left(1-\frac{J_1(2|\underline{q}|a)}{|\underline{q}|a}\right)\left(1-\frac{J_1(2|\underline{k}-\underline{q}|a)}{|\underline{k}-\underline{q}|a}\right). \quad \text{(B1)}$$

Defining $q\equiv|\underline{q}|$ and $p\equiv|\underline{k}-\underline{q}|$ we rewrite the integral as

$$\mathcal{I}=\int \frac{J(p,q)dpdq}{q^2p^2}\left(1-\frac{J_1(2qa)}{qa}\right)\left(1-\frac{J_1(2pa)}{pa}\right), \tag{B2}$$

where the Jacobian $J(p,q)$ is given by (see [8,22])

$$J(p,q)=2\pi pq\int_0^\infty bdbJ_0(bk)J_0(bq)J_0(bp), \tag{B3}$$

with $k=|\underline{k}|$. Inserting Eq. (B3) into Eq. (B2) we obtain

$$\mathcal{I}=2\pi\int_0^\infty bdbJ_0(bk)\left[\int_0^\infty\frac{dq}{q}J_0(bq)\left(1-\frac{J_1(2qa)}{qa}\right)\right]^2. \tag{B4}$$

The integration over p in Eq. (B2) is identical to the integration over q, which allowed us to square the q integral in Eq. (B4). Performing the integral in the square brackets we get (see [8,22])

$$\int_0^\infty\frac{dq}{q}J_0(bq)\left(1-\frac{J_1(2qa)}{qa}\right)=\theta(2a-b)\left[\ln\left(\frac{2a}{b}\right)-\frac{1}{2}+\frac{b^2}{8a^2}\right], \tag{B5}$$

which yields, for the original integral,

$$\mathcal{I}=2\pi\int_0^{2a}bdbJ_0(bk)\left[\ln\left(\frac{2a}{b}\right)-\frac{1}{2}+\frac{b^2}{8a^2}\right]^2$$
$$=2\pi(2a)^2\int_0^1 tdtJ_0(2akt)\left(\ln t+\frac{1}{2}(1-t^2)\right)^2, \tag{B6}$$

with $t=b/2a$. The integral in Eq. (B6) can be calculated by expanding the Bessel function in a power series, performing the integration in each term, and finally resumming the series. The result is

$$\mathcal{I}=2\pi a^2\left(-\frac{1+(ka)^2}{(ka)^4}[1-J_0(2ka)]+\frac{2+(ka)^2}{(ka)^4}J_2(2ka)\right.$$
$$\left.+{}_2F_3(1,1;2,2,2;-k^2a^2)\right). \tag{B7}$$

This expression is used to obtain Eq. (44). Taking the $k\to0$ limit of formula (B7) we obtain the integral appearing in the number of elastic scattering events [Eq. (42)]:

$$\int\frac{d^2\underline{q}}{(\underline{q}^2)^2}\left(1-\frac{J_1(2|\underline{q}|a)}{|\underline{q}|a}\right)^2=\frac{5}{6}\pi a^2. \tag{B8}$$

[1] J. W. Harris and B. Müller, Annu. Rev. Nucl. Part. Sci. **46**, 71 (1996).
[2] M. Gyulassy, Nucl. Phys. **A590**, 431c (1995).
[3] E. Shuryak, Phys. Rev. Lett. **68**, 3270 (1992); K. J. Eskola and M. Gyulassy, Phys. Rev. C **47**, 2329 (1993).
[4] B. Müller, Rep. Prog. Phys. **58**, 611 (1995).
[5] F. Karsch, Nucl. Phys. (Proc. Suppl.) **B34**, 63 (1994); Phys. Rev. D **49**, 3791 (1994); E. Laermann, Nucl. Phys. **A610**, 1c (1996).
[6] K. Geiger and B. Müller, Nucl. Phys. **B369**, 600 (1992); X. N. Wang and M. Gyulassy, Phys. Rev. D **44**, 3501 (1991); **45**, 844 (1992); Phys. Rev. Lett. **68**, 1480 (1992); Phys. Lett. B **282**, 466 (1992); Comput. Phys. Commun. **83**, 307 (1994).
[7] L. McLerran and R. Venugopalan, Phys. Rev. D **49**, 2233 (1994); **49**, 3352 (1994); **50**, 2225 (1994).
[8] A. H. Mueller, Nucl. Phys. **B415**, 373 (1994); **B437**, 107 (1995); A. H. Mueller and B. Patel, *ibid.* **B425**, 471 (1994).
[9] A. Kovner, L. McLerran, and H. Weigert, Phys. Rev. D **52**, 6231 (1995); **52**, 3809 (1995).
[10] J. Jalilian-Marian, A. Kovner, L. McLerran, and H. Weigert, Phys. Rev. D **55**, 5414 (1997); J. Jalilian-Marian, Report No. hep-ph/9609350, 1996.
[11] Yu. V. Kovchegov, Phys. Rev. D **54**, 5463 (1996).
[12] Yu. V. Kovchegov, Phys. Rev. D **55**, 5445 (1997).
[13] J. Jalilian-Marian, A. Kovner, A. Leonidov, and H. Weigert, Report No. hep-ph/9701284, 1997.
[14] J. F. Gunion and G. Bertsch, Phys. Rev. D **25**, 746 (1982).
[15] S. K. Wong, Nuovo Cimento A **65**, 689 (1970).
[16] C. Itzykson and J.-B. Zuber, *Quantum Field Theory* (McGraw-Hill, New York, 1985).
[17] L. N. Lipatov, Nucl. Phys. **B365**, 614 (1991); T. Jaroszewicz, Acta Phys. Pol. B **11**, 965 (1980).
[18] I. S. Gradshteyn and I. M. Ryzhik, *Table of Integrals, Series, and Products* (Academic Press, San Diego, 1980), Eqs. (8.411.1) and (6.561.5).
[19] M. Gyulassy and L. McLerran, Report No. nucl-th/9704034, 1997.
[20] J. D. Bjorken, Phys. Rev. D **27**, 140 (1983).
[21] B. Müller and D. H. Rischke (unpublished).
[22] E. T. Whittaker and G. N. Watson, *A Course of Modern Analysis* (Cambridge University Press, London, 1963), pp. 383–385.